Zinc electrode shape change II. Process and mechanism

redistribution of zinc material over the electrode, and so, shape change of the zinc electrode, can be monitored *in situ*. The results display that during repeated cycling zinc material is displaced gradually from the top towards the bottom of the electrode.

The mercury radiotracer experiments clearly indicate that mercury is not displaced over the zinc electrode during cycling of the battery.

Acknowledgments

The authors wish to thank Mrs. C. Zegers (IRI, Delft) for the radiochemical analysis of the many electrode samples and the staff of the SBD (TUE, Eindhoven) for technical consultations and for assistance with the radiochemical experiments.

Manuscript submitted June 29, 1989; revised manuscript received May 13, 1990.

Eindhoven University of Technology assisted in meeting the publication costs of this article.

REFERENCES

1. D. Hamby, J. Kucera, E. Miller, and N. J. Hover, in "Transport Processes in Electrochemical Systems," (PV 82-10) R. S. Yeo, T. Katan, and D.-T. Chin, Editors, p. 244, The Electrochemical Society Softbound Proceedings Series, Pennington, NJ (1982).
2. J. J. Lander and J. E. Cooper, Report AFAPL-TR-71-32, Wright-Patterson Air Force Base, OH (1971).
3. K. W. Choi, D. N. Bennion, and J. Newman, *This Journal*, **123,** 1616 (1976).
4. D. C. Hamby, N. J. Hoover, J. Wirkkala, and D. Zahnle, *ibid.*, **126,** 2110 (1979).
5. J. Hendrikx, Ph.D. Thesis, Eindhoven University of Technology, Eindhoven (1984).
6. R. G. Gunther and R. M. Bendert, *This Journal*, **134,** 782 (1987).
7. S. P. Poa and G. H. Wu, *J. Appl. Electrochem.*, **8,** 427 (1978).
8. J. McBreen, *This Journal*, **119,** 1620 (1972).
9. R. E. F. Einerhand, W. Visscher, E. Barendrecht, and J. J. M. de Goeij, in Vol. II, p. 751, Extended Abstracts of the 38th ISE Meeting, Maastricht (1987).
10. E. H. Hietbrink and R. F. Hill, *This Journal*, **136,** 310 (1989).
11. A. Himy and O. Wagner, in "Proceedings of the 28th Power Sources Conference," Atlantic City, NJ, June 12-15, 1978, The Electrochemical Society, Inc., p. 167.
12. J. McBreen and E. Gannon, *Electrochim Acta*, **26,** 1439 (1981).
13. A. Himy and R. Karcher, Abstract 90, p. 246, The Electrochemical Society Extended Abstracts, Vol. 80-2, Hollywood, FL, Oct. 5-10, 1980.
14. R. E. F. Einerhand, Ph.D. Thesis, pp. 118-127, Eindhoven University of Technology, Eindhoven (1989).
15. R. E. F. Einerhand, W. Visscher, J. J. M. de Goeij, and E. Barendrecht, *This Journal*, **138,** 7 (1991).
16. T. P. Dirkse, L. A. van der Lugt, and N. A. Hampson, *This Journal*, **118,** 1606 (1971).
17. J. McBreen and E. Gannon, *ibid.*, **130,** 1980 (1983).
18. J. McBreen and E. Gannon, *J. Power Sources*, **15,** 169 (1985).
19. R. E. F. Einerhand, Ph.D. Thesis, Chap. 4, pp. 48-82, Eindhoven University of Technology, Eindhoven (1989).
20. L. S. Melnicki, I. Lazic, and D. Cipris, *Final Report*, N00014-82-c-0701, Morristown, NY (1985).

Zinc Electrode Shape Change

II. Process and Mechanism

R. E. F. Einerhand[1] and W. Visscher

Laboratory for Electrochemistry, Eindhoven University of Technology, 5600 MB Eindhoven, The Netherlands

J. J. M. de Goeij

Laboratory for Instrumental Analysis, Eindhoven University of Technology, 5600 MB Eindhoven, The Netherlands and Interfaculty Reactor Institute, Delft University, 2629 JB Delft, The Netherlands

E. Barendrecht

Laboratory for Electrochemistry, Eindhoven University of Technology, 5600 MB Eindhoven, The Netherlands

ABSTRACT

The process and mechanism of zinc electrode shape change is investigated with the radiotracer technique. It is shown that during repeated cycling of the nickel oxide/zinc battery zinc material is transported over the zinc electrode via the battery electrolyte. During charge as well as during discharge zinc material is transported over the electrode. The direction of the zinc material transport during charge is opposite its direction during discharge. The amount of zinc material displaced over the electrode during charge is smaller than during discharge, so that after one charge-discharge cycle the net zinc material transport is observed in the direction as found during discharge. A new model for shape change is presented: the density gradient model. The model is based on the occurrence of an electrolyte flow during repeated charge-discharge cycling of the zinc secondary battery, which transports zinc material over the electrode. During battery cycling this electrolyte flow arises as a result of density gradients in the solution layer adjacent to the zinc electrode and of volume variations of the battery electrolyte.

The principal failure mode of nickel oxide/zinc secondary batteries is the gradual degradation of the zinc electrode, mainly as a result of the redistribution of zinc material over the electrode during repeated charge-discharge cycling, *i.e.*, zinc electrode shape change. Two models for zinc electrode shape change have been developed: the membrane pumping model, due to Choi *et al.* (1), and the concentration cell model, due to the McBreen (2). Choi *et al.* (1) state that electro-osmosis and osmosis cause forced convection in the zinc electrode compartment. The properties of the membrane separator, usually a weak cationic membrane, the presence and relative position of an electrolyte reservoir and the electrolyte between the battery plates determine the direction and rate of this convective flow. The changes in zincate concentration and flow direction during the charge and discharge half-cycles result in a net movement of zinc species in the direction

[1] Present address: Philips Research Laboratories, 5600 JA Eindhoven, The Netherlands.

parallel to the zinc electrode surface and away from the electrolyte reservoir.

McBreen (2) ascribes the occurrence of shape change to the discharge of concentration cells over the zinc electrode, arising from the nonuniform current density distribution and the different polarizability of the electrode during the charge and discharge processes. The model predicts a net movement of zinc material from the edges towards the center of the electrode. Experimental data on shape change (1-5) have not supported uncontested evidence in favor of one of these models. Choi's membrane pumping model cannot explain the occurrence of shape change when membrane separators are omitted. The induction of concentration cells in zinc secondary batteries with an applied nonuniform current density distribution (5), has revealed that concentration cells are not solely, if at all, responsible for the redistribution of zinc over the electrode.

Apart from the two often cited models for shape change (1, 2) a third model may be proposed: a model based on density gradients along and perpendicular to the zinc electrode surface. However, generally, diffusion and natural convection are considered to be relatively slow processes and are believed to be too slow to be responsible for the occurrence of shape change (1, 2, 5). It has also been argued, that density gradients along and perpendicular to the zinc electrode surface cannot explain the shape change behavior (1, 2, 5), since zinc secondary batteries operating in the horizontal mode showed shape change as well. However, it must be pointed out that the presence of an electrolyte reservoir can cause an electrolyte flow as a result of density gradients between electrolyte in the reservoir and in the zinc electrode compartment. This flow results in a net transport of zinc species over the electrode, away from the electrolyte reservoir and parallel to the zinc electrode surface, as will be discussed in this paper.

It was demonstrated in part I (6) that the movement of zinc over the electrode surface during repeated cycling can be monitored *in situ* with the radiotracer technique. Here, the process and mechanism of shape change will be investigated. For this purpose batteries were used which contain electrodes with radioactive material concentrated on a small part of the electrode. With these spot electrodes the movement of zinc material over the electrode can be studied at the start of the cycling experiment (7, 8), so the direction of zinc material transport and the amount of zinc material involved in the transport process can be determined. However, since the specific radioactivity over these electrodes does not remain constant throughout the cycling process, these electrodes cannot be used to monitor zinc electrode shape change *in situ*.

Experimental

The preparation of the PTFE-bonded zinc oxide electrodes as well as the cell assembly, battery cycling regimen, and experimental setup for the radioactivity measurements are described in part I (6).

The spot electrodes, *i.e.*, electrodes with a small radioactive (^{65}Zn) part, are prepared with nonradioactive PTFE-bonded zinc oxide over the total electrode surface, except that 10-25 mm^2 of the electrode is covered with 10-100 mg radioactive PTFE-bonded zinc oxide, with a specific radioactivity of about 50 GBq · kg^{-1}. The spot was positioned at a single region on the electrode. The experiments are carried out using vertical cells (V-cell, internal dimensions, $h \times l \times w$, 100 × 37 × 4 mm) and horizontal cells (H-cell, internal dimensions, 4 × 37 × 57 mm) in which the electrodes are placed both parallel and perpendicular to the earth's gravitational field, respectively. The H cell has a small opening at the side of the electrolyte reservoir, so that gas produced at the electrodes cannot escape readily, as is the case with the V cell.

At the end of the cycling regimen, prior to scraping from the zinc electrode, electrode-mass samples (10 mm^2, 1-7 mg) are taken from the midst of each region and from the corners of the center region (a total of 13 samples). These samples are examined for their radioactivity, specific radioactivity and zinc and PTFE content. Further analysis of the zinc electrode is described in part I (6).

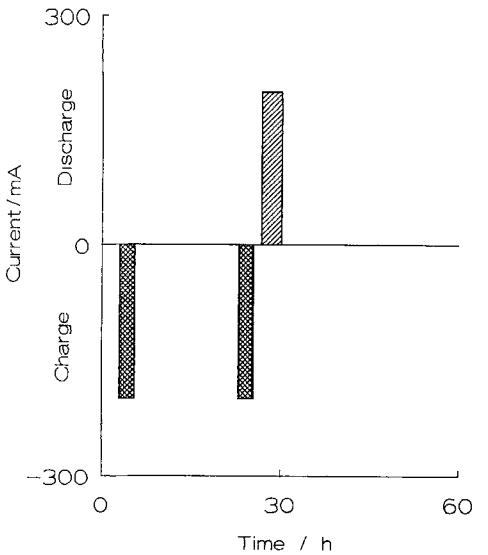

Fig. 1. Current regime for the battery with a spot electrode, subjected to one charge-discharge cycle (V cell).

Results

^{65}Zn distribution during one charge-discharge cycle, V-cell.—The movement of the radiotracer over a freshly prepared electrode during one charge-discharge cycle is studied, using an electrode with a radioactive spot located at region I (cf. Fig. 3 in part I (6)). The current-time regime imposed upon the battery is presented in Fig. 1. To investigate the change of the radioactivity distribution when the electrolyte is severely depleted in reducible zinc species, two consecutive charge periods were introduced. The total charge time is twice the charge time used in the cycling experiments. The charge process is interrupted for 18h to monitor the movement of the radiotracer over the (partially) charged electrode. The radioactivity of the spot is measured over more than six months after the discharge period.

Figure 2 shows the change in radioactivity of the radioactive spot with time, measured with the conical collimator. At the end of the first charge period the radioactivity distribution is virtually unaltered. After the 18h rest period, a significant decrease is observed. During the second charge period the radioactivity at the spot alters marginally, whereas during the discharge half-cycle the radioactivity shows a sharp decrease.

The battery remains at open-circuit potential over more than six months. Figure 2 shows that the radioactivity of the spot decreases continuously during this period, though the rate of decrease gradually diminishes at longer time intervals.

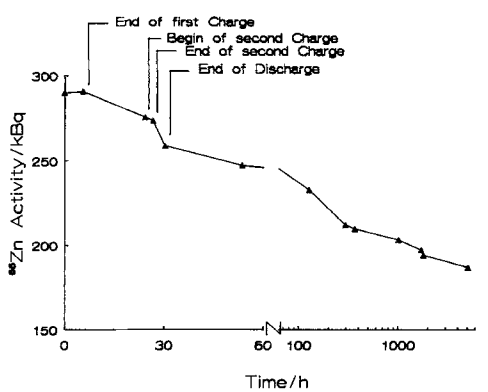

Fig. 2. The change in radioactivity at region I of an electrode having a radioactive spot at region I. The current regime imposed upon the battery is depicted in Fig. 1. The abcisses is broken in two parts with different scales.

^{65}Zn distribution over a spot electrode during repeated cycling, V cell.—Batteries are assembled in vertical cells using electrodes with a spot positioned at a particular region of the electrode. During repeated cycling the radioactivity over the electrode is monitored with the conical collimator. The results for a battery with an electrode with a spot located at region III are given in Fig. 3. The radioactivity of the spot decreases right from the beginning of the experiment. At almost all the other positions an increase in radioactivity is observed, which is most markedly observed at the positions beneath the radioactive spot. At the end of battery cycle life, changes in the distribution of the radioactivity over the electrode are small.

It is observed that during repeated cycling, irrespective of the position of the spot, its radioactivity decreases. The radioactivity at the positions beneath the radioactive spot increases more than at other positions. Positioning of the spot at the bottom of the electrode results in a more gradual and less pronounced change of the radioactivity distribution.

^{65}Zn distribution over a spot electrode during repeated cycling, H cell.—A second series of cycling experiments is carried out with spot electrodes arranged in horizontal cells using the rectangular collimator. The capacity of such batteries tends to decrease more slowly than the capacity of batteries in vertical cells. Generally, a longer cycle life was found for batteries in horizontal cells than for batteries in vertical cells.

The radioactivity distribution during the cycling test is shown in Fig. 4, for an electrode with the spot located at region VII. Analogous to the findings with vertical cells, the radioactivity at the spot decreases and the radioactivity at all other positions increases. The radiotracer moves in all directions, like in vertical cells. The regions gaining the most radioactivity during the cycling process are the nearby regions IV, V, and VIII.

Ex situ analysis of the zinc electrode, V-cell.—In Fig. 5 the percentual electrode-mass distribution is presented for a zinc electrode cycled 100 times in a vertical cell. The average percentage electrode mass in a region for a freshly prepared electrode is theoretically 11.1%. Hence, evidently, shape change has occurred. For each sample the zinc and PTFE content, as well as the specific radioactivity, were determined. It was found that the amount of PTFE per region over the electrode was nearly equal over the electrode and close to the theoretically expected value. The zinc content of the electrode mass of each region, relative to the overall zinc content of the total electrode mass, is given in Fig. 6. These numbers are calculated using the formula

$$X_j = \frac{M_{Zn,j}/M_{El,j}}{\sum_{i=1}^{n} M_{Zn,i} \Big/ \sum_{i=1}^{n} M_{El,i}}$$

where $M_{Zn,j}$ and $M_{Zn,i}$ represent the zinc mass and $M_{El,j}$ and $M_{El,i}$ the electrode mass at a particular region on the electrode. The summation is performed over the nine regions on the electrode. Hence, X_j smaller than unity indicates that the zinc content of the electrode mass is smaller than the zinc content of the total electrode mass. The zinc content at the top regions is considerably lower than at the bottom regions. This must be the result of the transport of zinc material during battery cycling from the top towards the bottom of the electrode.

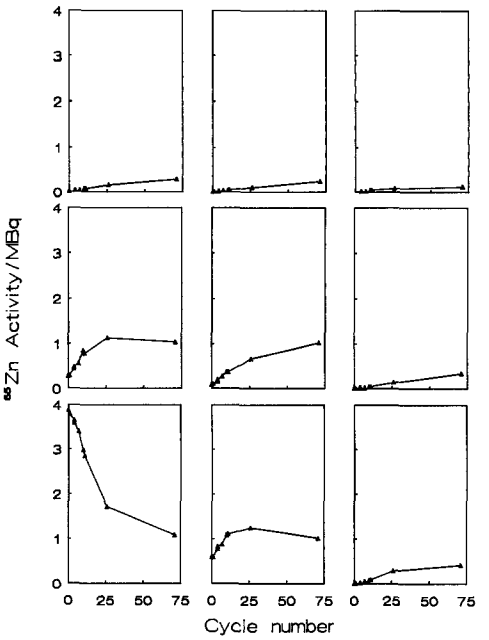

Fig. 4. The change in radioactivity at the nine regions of the electrode [cf. Fig. 3 in part I (6)] during cycling of a battery with a spot electrode in a vertical cell. The spot is placed at region VII.

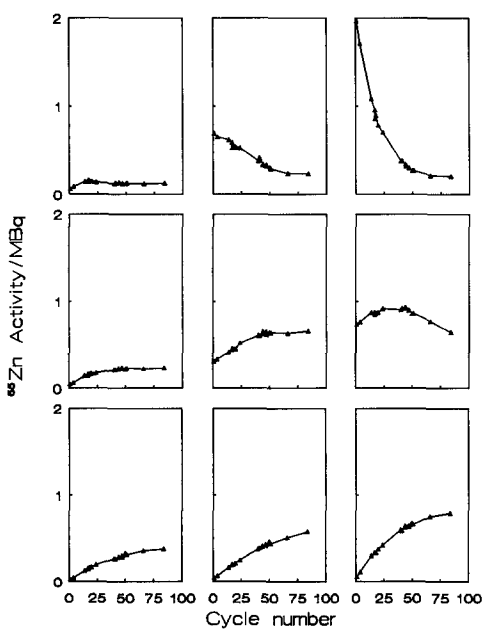

Fig. 3. The change in radioactivity at the nine regions of the electrode [cf. Fig. 3 in part I (6)] during cycling of a battery with a spot electrode in a vertical cell. The spot is placed at region III.

3.3	4.3	2.0
6.8	16.5	6.6
24.6	25.5	10.4

Fig. 5. Relative electrode mass distribution at the nine regions of the zinc electrode cycled in a vertical cell, after 100 cycles.

Fig. 6. Zinc content at the nine regions of the zinc electrode relative to the zinc content of the total electrode mass, for the electrode cycled in a vertical cell.

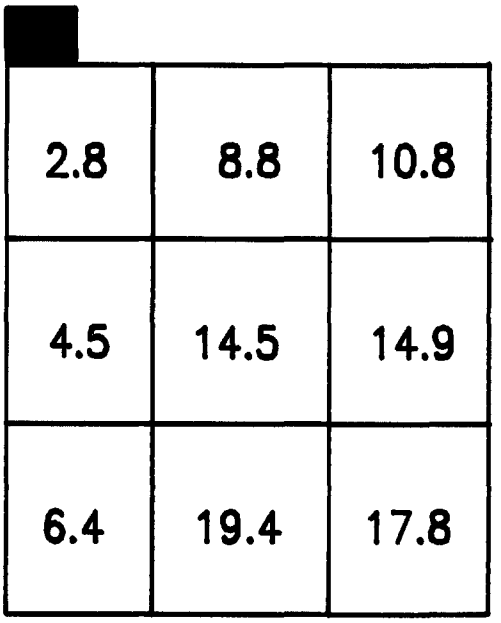

Fig. 8. Relative electrode mass distribution at the nine regions of the zinc electrode for the electrode cycled in a horizontal cell, after 52 cycles.

The specific radioactivity of each sample relative to the specific radioactivity of the total electrode mass is given in Fig. 7, and is calculated from

$$Y_j = \frac{A_{Zn,j}/M_{Zn,j}}{\sum_{i=1}^{n} (M_{El,i} \cdot A_{Zn,i}/M_{Zn,i}) \Big/ \sum_{i=1}^{n} M_{El,i}} \quad [2]$$

$A_{Zn,j}$ and $A_{Zn,i}$ represent the ^{65}Zn radioactivity (Bq) of the electrode mass scraped from regions j and i, respectively. The electrode originally had a spot located at region III. At the end of the battery cycle life the highest specific radioactivity is still found at region III, as can be seen from Fig. 7. The regions beneath the radioactive spot show a significantly higher specific radioactivity than the other regions. This clearly indicates that in vertical cells, zinc materials is transported predominantly from the top towards the bottom of the electrode.

Ex situ analysis of the zinc electrode, H-cell.—The percentual electrode mass distribution of an electrode, with a spot located at region I and cycled 52 times in a horizontal cell, is given in Fig. 8. It can be seen that regions I, II, IV, and VII lost, and regions V, VI, VII, and IX gained zinc material. Figure 8 shows that apart from zinc material transport from the regions nearest the electrolyte reservoir ("top" regions) towards the regions farthest away from the electrolyte reservoir ("bottom" regions), zinc material is also transported from one side of the electrode to the other. This was occasionally observed with other electrodes and also with electrodes cycled in vertical cells. Most likely, this is the result of imperfect alignment of the electrodes in the battery.

The distribution of zinc over the electrode can be observed in greater detail from Fig. 9, where the zinc content in each sample, relative to the total zinc content in all samples, is presented. The numbers are calculated analo-

Fig. 7. The specific radioactivity at the nine regions of the zinc electrode relative to the specific radioactivity of the total electrode mass, for the electrode cycled in a vertical cell. The spot is placed at region III.

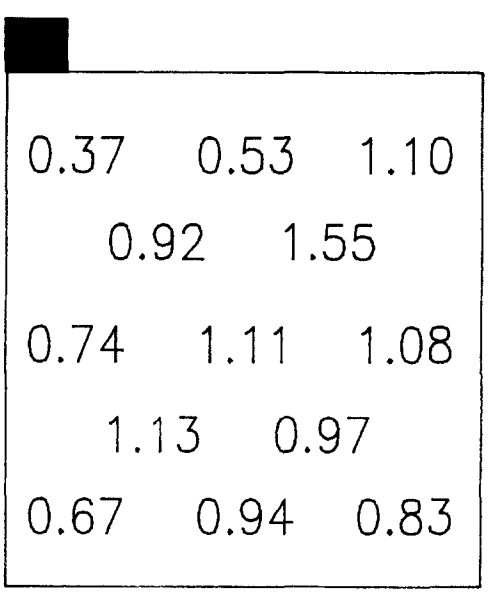

Fig. 9. Zinc content at 13 points of the zinc electrode relative to the total zinc content of all samples, for the electrode cycled in a horizontal cell.

gous Eq. [1], in which the summation now is performed over the 13 samples, M_{Zn} refers to the zinc mass in the sample and M_{El} to the sample mass. From this figure, it can be deduced that zinc material is transported towards the center region but also towards regions III, VI, VII, and IX. Zinc material is supplied predominantly by regions I and II and to a minor extent by regions IV and VII.

The specific radioactivity over the electrode is determined for the 13 samples. The ratio of the specific radioactivity of the individual samples to the specific radioactivity of the sum of all samples is presented in Fig. 10. The numbers are calculated analogous to Eq. [2], in which the summation now is performed over the 13 samples, and A_{Zn} refers to the ^{65}Zn radioactivity of the sample, M_{Zn} to the zinc mass in the sample and M_{El} to the sample mass. The electrode is prepared with a spot located at the lower right-hand corner of region I. As was observed with the electrode cycled in a vertical cell, at the end of battery cycle life the specific radioactivity is still highest at the spot position. Also, moving away from the spot position, the specific radioactivity decreases, which is observed also with the vertical cell experiment (cf. Fig. 7). Figure 10 shows that the transport of the radiotracer is predominantly downwards, *i.e.*, from the top towards the bottom of the electrode. However, it can be inferred also from Fig. 10, that the zinc material transport from the left towards the right-hand side of the electrode, contributes substantially to the total zinc material transport.

Discussion

The dissolution/precipitation vs. direct zinc electrode reaction.—During the discharge process zinc oxide can be formed directly or via the formation and subsequent disproportionation of zincate ions. The experiment with a spot electrode which is charged and discharged only once, can provide information on the course of the zinc electrode reaction. Figure 2 demonstrates that during both charge periods the radioactivity of the radioactive spot remains virtually constant. This indicates that radioactive zinc oxide is reduced at the spot location self. Most likely, no soluble intermediates are formed, *i.e.*, zinc oxide is reduced directly, since if radioactive zincate ions are produced during the charge process, it is expected that these ions will be transported over the electrode surface.

During the discharge process the radioactivity of the spot decreases significantly (cf. Fig. 2). The anodic zinc electrode reaction produces zincate ions which are readily transported over the zinc electrode. Hence, during discharge the dissolution/precipitation path prevails.

The results given in Fig. 2 indicate moreover that zinc corrosion occurs when the battery is charged and remains at open-circuit potential. During the rest period, in between charge periods and after battery discharge the radioactivity of the radioactive spot decreases. This decrease is due to the displacement of the radiotracer over the electrode. Since initially radioactive zinc is absent in solution and since zinc oxide does not dissolve readily in the battery electrolyte (6), the formation of radioactive zincate ions in solution must be attributed to corrosion of zinc.

Direction of ^{65}Zn transport during battery cycling.—The direction of the transport processes during charge and discharge can be obtained from experiments with spot electrodes. A change of the radioactivity over the zinc electrode will be the result of the movement of radioactive zincate ions in solution. The movement of the radiotracer, though to a minor extent also caused by interdiffusion of radioactive and nonradioactive zincate ions, indicates the direction and amount of zinc material involved in the shape change process.

From the measurement of the specific radioactivity at the end of the cycling regimen, cf. Fig. 7 and 10, it can be deduced that in vertical as well as in horizontal cells, the net zinc material transport is predominantly from the top towards the bottom regions. For the electrode cycled in a horizontal cell, the substantial zinc material transport from the left towards the right-hand side of the electrode can be explained with the nonalignment of the counter- and zinc electrodes, as has been reported by McBreen and Cairns (9).

The spot electrode subjected to one charge-discharge cycle in the V cell, showed a marked decrease in radioactivity at the spot region after one cycle (cf. Fig. 2). For this electrode, the amount of radioactive material transported from the spot towards other regions on the electrode, relative to the amount lost at the spot region, is given in Fig. 11. The regions beneath the radioactive spot receive 65% of the amount of radioactive material lost at the spot. All other regions gain a considerably smaller amount of radioactive material, of which the regions nearest the radioactive spot gain more than those farther away. Since the radioactive spot shows the most marked decrease of radioactivity during discharge, it follows that radioactive zinc material moves downwards during discharge.

The displacement of the radiotracer during charge cannot be obtained from this experiment since during the

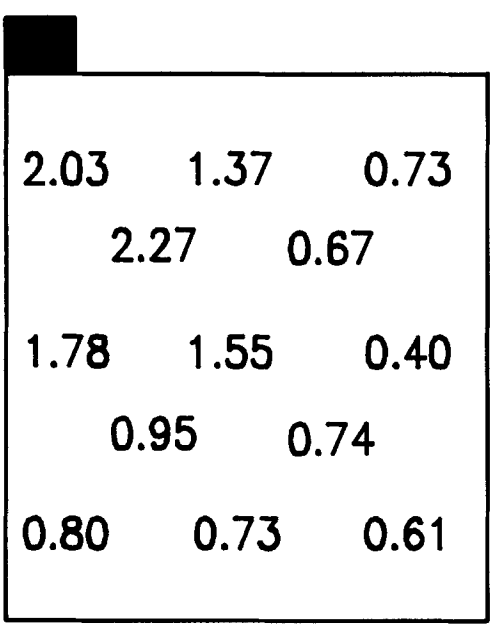

Fig. 10. The specific radioactivity at 13 points of the zinc electrode relative to the specific radioactivity of all samples, for the electrode cycled in a horizontal cell.

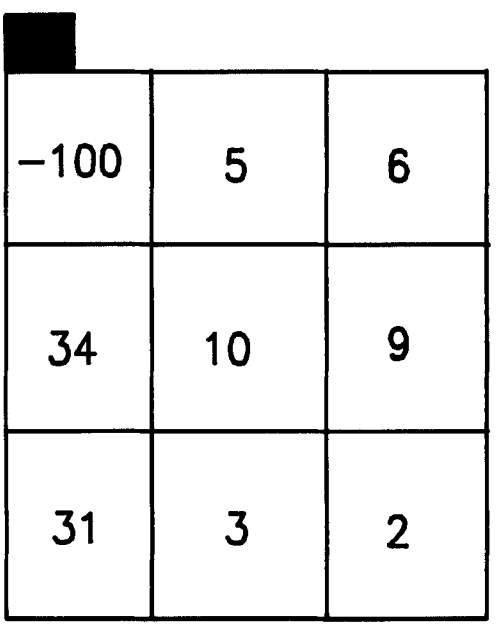

Fig. 11. The transport of radioactive material from region I towards other regions, for the electrode subjected to one charge-discharge cycle. The decrease of the radioactivity at region I is set at 100% and the radioactivity increase at other regions is given relative to the decrease at region I.

charge half-cycle the radiotracer is concentrated on the electrode and does not dissolve into the electrolyte. However, this does not mean that during charge zinc material will not be displaced over the electrode. The direction of the net zinc material movement during charge and discharge can be obtained from the cycling experiment with an electrode of uniform specific radioactivity. The radioactivity data of the three top regions [see Fig. 5 in part I, (6)] are totaled and replotted in Fig. 12 for cycles 11, 22, and 49. Figure 12 shows the change in radioactivity relative to the radioactivity at the beginning of a cycle (note that the measurements are made during the rest period between subsequent half-cycles). The radioactivity at the top of the electrode has increased at the end of the charge period. A decrease, usually larger than the previous increase during charge, is observed during the subsequent discharge period. Consequently, the net transport of the radiotracer over the electrode is in the direction of the movement of the radiotracer during discharge. For the same electrode, the change in radioactivity at the bottom positions is depicted in Fig. 13 for cycles 11, 22, 49. The radiotracer is transported towards the bottom of the electrode during the discharge half-cycle, and is transported in the opposite direction during the charge half-cycle.

For horizontal cells the direction of the zinc material transport over the zinc electrode can also be obtained from data of electrodes of uniform specific radioactivity. The radioactivity data at the regions nearest the electrolyte reservoir, the top regions, are summed and plotted in Fig. 14, relative to the beginning of a cycle for cycles 11, 22, and 49. Generally, the radiotracer is transported away from the top regions during discharge and towards these regions during charge. From Fig. 15 it can be observed that the radiotracer is transported away from the regions farthest from the electrolyte reservoir, the bottom regions, during charge and towards these bottom regions during discharge. Thus, analogous to the findings with vertical cells, radioactive zinc material is transported from the bottom towards the top of the electrode during charge and in the opposite direction during discharge.

Thus, it appears that zinc material is continuously being transported over the electrode, the direction of this transport is reversed when the electric current is reversed.

From experiments with ^{137}Cs added as a radiotracer to the battery electrolyte, Hietbrink and Hill observed that the electrolyte is transported out of the electrode pack during charge and into the electrode pack during discharge (8). They concluded that the direction of the zinc material transport is mainly from the edges towards the center of the electrode, and to a lesser extent from the top towards the bottom of the electrode. However, their radiotracer experiments with ^{65}Zn clearly indicated that during cycling zinc material is transported from the top towards the bottom of the electrode.

The zinc material displacement rate.—The amount of zinc material displaced over the electrode can be obtained from experiments with spot electrodes and from experi-

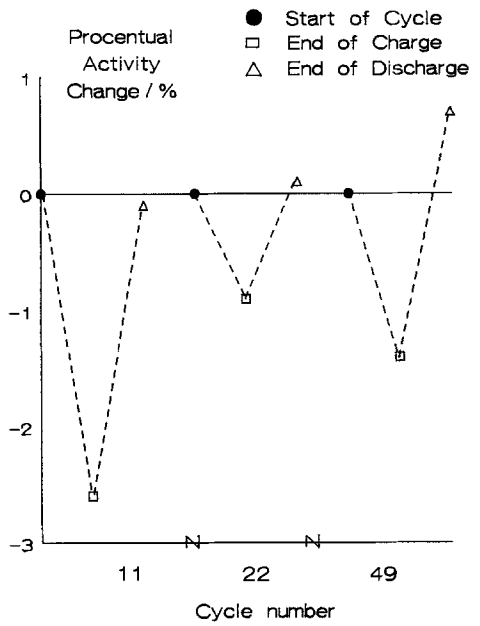

Fig. 13. The percentage change in radioactivity at the bottom regions at the end of the charge and discharge period relative to the start of the cycle 11, 22, and 49. The data have been collected from the cycling experiment of an electrode with uniform specific radioactivity in a vertical cell [cf. Fig. 5 in part I (6)]. Symbols as given in the Fig. 12 caption.

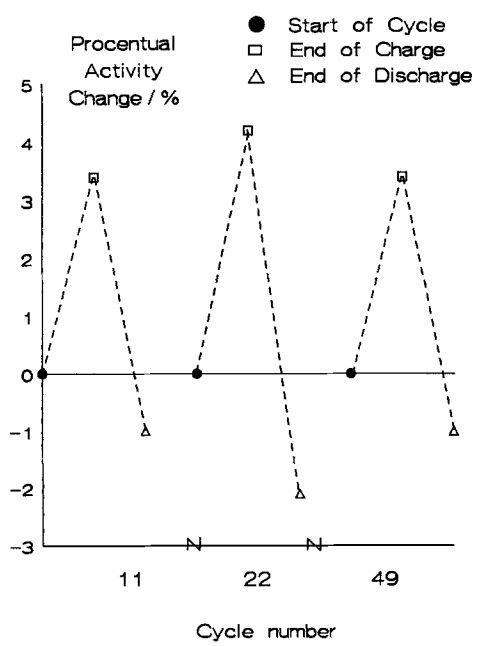

Fig. 12. The percentage change in radioactivity at the top regions at the end of the charge and discharge period relative to the start of the cycle 11, 22, and 49. The data have been collected from the cycling experiment of an electrode with uniform specific radioactivity in a vertical cell [cf. Fig. 5 in part I (6)]. Closed circle: start of cycle; open square: end of charge; open triangle: end of discharge.

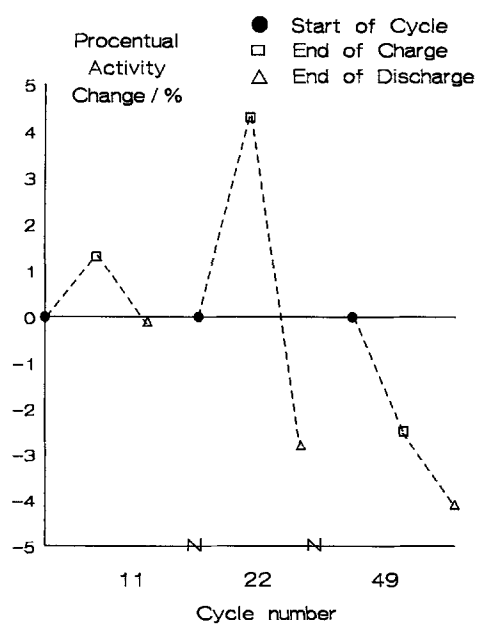

Fig. 14. The percentage change in radioactivity at the regions nearest the electrolyte reservoir at the end of the charge and discharge period relative to the start of the cycle 11, 22, and 49. The data have been collected from a cycling experiment of an electrode with uniform specific radioactivity in a horizontal cell. Symbols as given in the Fig. 12 caption.

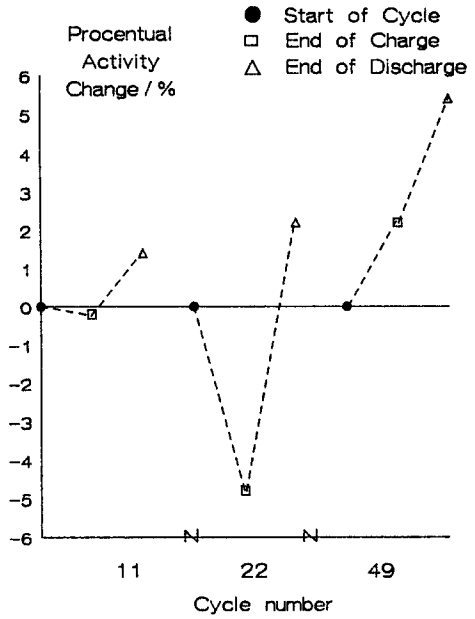

Fig. 15. The percentage change in radioactivity at the regions farthest away from the electrolyte reservoir at the end of the charge and discharge period relative to the start of the cycle 11, 22, and 49. The data have been collected from a cycling experiment of an electrode with uniform specific radioactivity in a horizontal cell. Symbols as given in Fig. 12 caption.

ments with electrodes of uniform specific radioactivity. At the beginning of battery cycling the transport of the radiotracer over the electrode differs when the radioactive spot is located at different regions on the electrode. During the first few cycles, in vertical cells, when the spot is located at the top positions, typically, a 7% radioactivity decrease per charge-discharge cycle is observed at the radioactive spot. When the spot is positioned at the center or bottom of the electrode a significantly lower percentage decrease is found: usually 2% per cycle. This marked difference in percentage decrease, when the radioactive spot is located at different positions, can be explained as follows. If the radioactive spot is at a top region during charge only nonradioactive zinc material is transported towards this region; during discharge zinc radioactive material is transported from this region towards the bottom of the electrode, as was pointed out in the preceding section. Thus, the radioactivity of the spot at the top of the electrode decreases chiefly during discharge. If the spot is positioned at the bottom of the electrode, nonradioactive material is transported towards the spot region during discharge and radioactive zinc material is transported away from the region during charge. Since, on average, the zincate concentration in the battery electrolyte is higher during discharge than during charge, the amount of radioactive zinc material transported over the electrode is larger during discharge than during charge.

The net zinc material transport can be estimated from the above percentages. Since the zinc material transport during charge amounts to 2% per cycle and during discharge to 7% per cycle, the net material transport is 5% per cycle. Of course, this percentage is only a very rough estimate of the net zinc material transport. Nevertheless, assuming a decrease of 5% per each cycle, at the top regions the radioactivity will have decreased with 25% after 5.6 cycles and with 50% after 13.5 cycles. From the results plotted in Fig. 5 of part I (6), it can be seen that the top of the electrode, after 5 or 6 cycles the radioactivity has decreased with 25% and, after 19 to 20 cycles, with 50%. Thus, only during the first few cycles an average decrease of 5% per cycle is observed. The net material transport decreases when cycling proceeds and an average 3.5% decrease per cycle is calculated when the radioactivity at the top positions has decreased with 50%.

At the beginning of cycling the three bottom positions gain an amount of radioactive material equal to the loss at the top positions. It can be observed from the results given in Fig. 5 of part I (6), that the positions VII and IX show by far the largest increase in radioactivity. At the start of the experiment a much smaller radioactivity is observed at these positions, particularly at position VII, than at position VIII. Probably, at the start of the cycling experiment, the zinc electrode thickness at these positions is smaller that at position VIII. The radioactive electrolyte transported towards the bottom positions during discharge can accumulate at these positions. Therefore, the radioactivity can rise appreciably at positions VII and IX. Thus, as has been shown in part I for the battery with only radioactive electrolyte (6), the presence and position of an electrolyte reservoir and of electrolyte between the battery plates is only of crucial importance for the material transport in the battery.

Similar calculations as above for experiments in horizontal cells lead to a calculated transport during charge of 1.5% and during discharge of 5.5%. On average, a net material transport of 4% is expected which is slightly lower than in vertical cells. This is in agreement with the findings of a battery with an electrode of uniform specific radioactivity cycled in a horizontal cell. The average decrease at positions near the electrolyte reservoir is about 4% per cycle and the average increase at the "bottom" regions about 5%, due to the decrease observed at the middle positions.

Thus, the longer useful cycle life of batteries operating in horizontal cells is likely to be due to the smaller amount of zinc material transported. Consequently, the shape change rate is smaller in horizontal cells than in vertical cells.

The shape change process and mechanism.—The results of our radiotracer experiments cannot be explained on the basis of McBreen's concentration cell model (2). McBreen states that at the beginning of cycling the nonuniform current density distribution over the electrode and the higher electrode polarizability during charge leads to a depletion of reducible zinc species at the edges of the electrode. If diffusion of zincate ions from the center towards the edges of the electrode cancels the concentration gradients, the radiotracer experiments should have shown an increasing radioactivity at the edge of the electrode. Since the current density is more non-uniform at the top of the electrode, the movement of the radiotracer should be predominantly in this direction. This is found with none of our experiments. McBreen suggested that diffusion processes are of minor importance and that the concentration gradients are canceled by concentration cells over the electrode surface. If so, it would imply that the radiotracer distribution should remain constant. This also is not observed in our experiments. Therefore, McBreen's concentration cell model is not applicable.

From the above experiments and from the experiments described in part I (6), it is deduced that the electrolyte flow in the battery is the principal mode of material transport in the battery. During discharge this flow transports zinc material from the top towards the bottom of the electrode; during charge zinc material is displaced in the opposite direction. Since the amount of zinc material involved in the displacement process is larger during discharge than during charge, a net zinc material transport is observed in the direction as observed during discharge, *i.e.*, from the top towards the bottom of the electrode.

The Density Gradient Model

It has not unambiguously been established that the driving forces as proposed by Choi and McBreen are indeed responsible for the shape change behavior of the zinc electrode. Choi *et al.* (4, 10) demonstrated that during battery operation an electrolyte flow arises in the zinc electrode compartment; but this does not prove that the observed electrolyte flow is indeed caused by electro-osmosis and/or osmosis. McBreen (2) showed that concentration cells may give rise to redistribution of zinc material over the electrode; but he failed to establish the origin and existence of such concentration cells in the battery, and its relation to the observed shape change pattern.

From results of our experiments it has become clear that shape change occurs, whether or not separators are implemented in the battery (11); an observation also reported by McBreen and Cairns (9). Also, we found that the zinc material transport in the battery is not as predicted by McBreen's concentration-cell model, *viz.*, from the edges towards the center of the electrode (6). Gunther and Bendert (5) also reported that a controlled nonuniform current density distribution did not result in zinc material transport as expected from McBreen's theory.

Therefore, we propose a new model for shape change: the density gradient model. In this model shape change results from the change in density and volume of the battery electrolyte during cycling, inducing a convective flow which transports zinc material over the electrode.

At present, a rigorous quantitative analysis of the system is impossible. Numerous assumptions are required due to the lack of experimental data (*e.g.*, the thermodynamics of the (supersaturated) zincate solutions, the hydrodynamics of electrolyte in small spaces with compressible and/or changing walls). Therefore, the model as presented here, is based on qualitative arguments.

The solution layer adjacent to the electrode.—During battery operation the composition of the battery electrolyte changes continuously. Since the properties of the battery electrolyte (*e.g.*, density, conductivity, viscosity) change markedly with varying solute concentration (12-14), they must also change during cycling of the battery. Consequently, concentration gradients and, therefore, density gradients develop perpendicular to the zinc electrode surface. As a consequence, a solution layer adjacent to the electrode with a density which differs from the density of the bulk electrolyte arises. This layer can extend gradually from within the porous electrode matrix to close to the separator, depending on the progress of the cycling process, the geometry of the cell and the properties of the electrolyte.

The diffusion coefficients of potassium and hydroxyl ions are considerably larger than that of zincate ions. Also, the separator, commonly used in batteries with zinc electrodes, strongly inhibits the migration and diffusion of zincate ions between zinc and counterelectrode compartment. Hence, concentration variations of potassium and hydroxyl ions will be considerably less pronounced than those of zincate ions. Hamby *et al.* (15) and Isaacson *et al.* (16) found indeed that the KOH concentration was approximately constant during cycling, but the zincate concentration decreases markedly during charge ($<0.1M$), and increased to about four times the ZnO solubility during discharge. We found (6) that during one cycle only about 0.1% of the radioactive zinc material is transported from the zinc electrode towards the nickel electrode compartment. Thus most likely, changes in the properties of the battery electrolyte in the zinc electrode compartment arise from variations in zincate ion concentration.

Vertical cells.—First, the movement of the solution layer during battery operation in vertical cells will be discussed. The earth's gravitational field is directed parallel to the zinc electrode surface and perpendicular to the density gradient. Hence, at a particular height in the cell, volume elements in the bulk and in the solution layer experience different forces, causing electrolyte movement.

The direction of the electrolyte flow as a result of the density gradient is parallel to the zinc electrode surface. During discharge the zincate concentration in the solution layer adjacent to the electrode is higher than the bulk zincate concentration. Since the density of the battery electrolyte increases markedly with increasing zincate concentration (13, 14), the solution layer adjacent to the electrode experiences a force directed towards the bottom of the electrode, resulting in an electrolyte flow, as is depicted schematically in Fig. 16. Consequently, during discharge electrolyte with a high concentration of zincate ions is transported from the top towards the bottom of the electrode.

During the charge period, the solution layer adjacent to the electrode becomes depleted in zincate ions and its density decreases. The electrolyte transport resulting from the charge process is directed from the bottom towards the top of the electrode. So, during charge, zincate ions are transported in the opposite direction as they are during discharge.

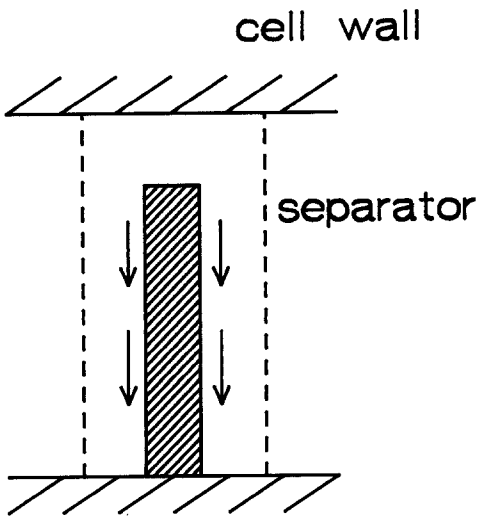

Fig. 16. Arrows indicate electrolyte movement in the zinc electrode compartment of a vertical cell as a result of density gradients for the zinc electrode being discharged.

The amount of zinc material involved in the displacement process is higher during discharge than during charge, because in the solution layer the concentration of zincate ions is much higher during discharge than during charge. Thus the net result of the zinc material transport due to natural convective transport during one charge-discharge cycle, is that zinc material agglomerates at the bottom of the electrode. This type of zinc material transport was found experimentally, as can be seen from the results given in Fig. 12 and 13.

During some stage of the discharge process, the battery electrolyte will become supersaturated with zinc material and precipitation of ZnO or related products can occur (depending on factors such as cell design, cycling regimen, battery electrolyte composition). Since a solution concentrated with zinc material is transported towards the bottom of the electrode, more zinc material will precipitate at the bottom than at the top of the electrode. (Note that at present the exact solubility limit, and the precipitation/dissolution rate of zinc material is unknown. Not even the nature of the zinc species in the supersaturated solution and of the species precipitating from these solutions is clear. Therefore, a quantitative determination of the time and location at which precipitation will occur is not possible.)

Usually, in vertical as well as horizontal cells some space is left over the top of the electrodes for excess electrolyte: an electrolyte reservoir. This electrolyte reservoir, depending on its size, influences the electrolyte flow in vertical cells. The larger the amount of electrolyte in the reservoir, the greater the supply of bulk electrolyte and the longer the time a large density gradient can exist. Thus, more zinc material can be transported during one-half cycle. Also, at the top of the electrode the supply of zincate ions is larger if more electrolyte resides over the top of the electrodes. Hence, the top regions will become depleted in zinc during a later stage of the cycling process.

Thus, if an electrolyte reservoir is present, the amount of zinc material involved in the displacement process can increase, but in vertical cells, shape change will occur, whether an electrolyte reservoir is present or not.

Horizontal cells without an electrolyte reservoir.—In horizontal cells the solution layer adjacent to the electrode and the bulk electrolyte will show a similar change in composition as observed in vertical cells. However, in horizontal cells the density gradient is directed parallel to the earth's gravitational field and, in the absence of an electro-

lyte reservoir at one side of the electrodes, electrolyte movement perpendicular rather than parallel to the zinc electrode surface occurs.

For the solution layer above the electrode, natural convection is expected to contribute insignificantly to mass transport during discharge, since the density of the solution layer adjacent to the electrode steadily increases. For the solution layer underneath the electrode, the density gradient induces electrolyte movement perpendicular to the zinc electrode surface: the solution layer "falls" from the electrode and is replaced with bulk electrolyte, as is shown schematically in Fig. 17. The concentration profiles will be, however, very irregular. Consequently, above the electrode zincate species are being precipitated onto the zinc electrode in an earlier stage of the discharge process than they are underneath the electrode. Also, underneath the electrode precipitation may occur at other places than onto the electrode. As a result, after discharge more reducible zinc species are present on top than underneath the electrode.

During charge the electrolyte layer above the electrode which is depleted in zincate ions, will move upwards, since its density is lower than that of the bulk electrolyte. Thus bulk electrolyte is transported towards the electrode, accelerating the diffusion of zincate ions. For the electrolyte layer underneath the electrode scarcely any movement of the electrolyte is expected and diffusion of zincate ions is the only mass transport mode. Therefore, it can be deduced that the zinc deposition rate is higher above than underneath the electrode. After one charge-discharge cycle, effectively, zinc material agglomerates above the electrode and disappears from underneath the electrode. This behavior was found indeed for almost all zinc electrodes cycled in the horizontal cell [see *e.g.*, Fig. 6, in (17)].

Horizontal cells with an electrolyte reservoir.—The above reasoning concerns electrolyte movement in the absence of an electrolyte reservoir. If, however, in the battery an electrolyte reservoir is present at one side of the electrode pack, additionally, an electrolyte flow parallel to the zinc electrode results (Fig. 18). This electrolyte flow is caused by volumetric changes of the electrolyte in the zinc electrode compartment and, to a much smaller extent, to density gradients.

To make this clear, let us consider the processes during one charge-discharge cycle. During discharge, the volume of the electrolyte in the zinc electrode compartment decreases due to changes of the solute concentration and the density of the electrolyte, as is demonstrated in the Appendix. This volume decrease causes an electrolyte flow from the electrolyte reservoir towards the zinc electrode compartment. This flow transports electrolyte, which is highly concentrated in zincate ions, away from the electrolyte reservoir into the zinc electrode compartment; thus causing zinc material to be displaced in the same direction. Taking the side of the zinc electrode close to the electrolyte reservoir as the top of the electrode and the other side as the bottom of the electrode, zinc material is transported from the top towards the bottom of the electrode.

During charge the volume of the electrolyte in the zinc electrode compartment increases (see Appendix) and electrolyte is pushed from the zinc electrode compartment

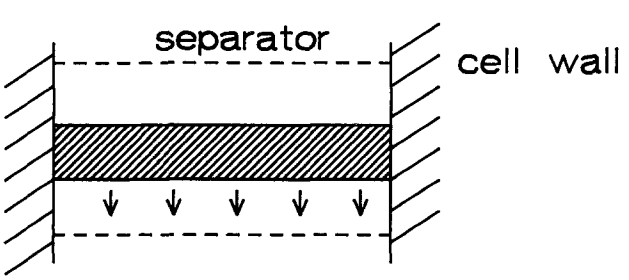

Fig. 17. Arrows indicate electrolyte movement in the zinc electrode compartment of a horizontal cell without an electrolyte reservoir as a result of density gradients, for the zinc electrode being discharged.

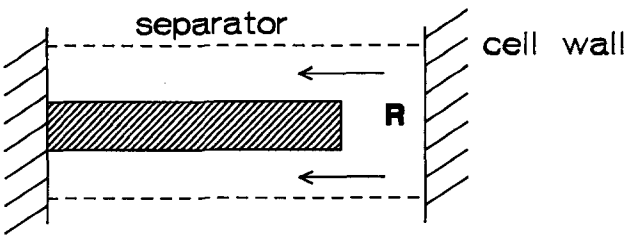

Fig. 18. Arrows indicate electrolyte movement in the zinc electrode compartment of a horizontal cell with an electrolyte reservoir at one side of the electrode pack (R), for the zinc electrode being discharged.

into the electrolyte reservoir. Thus, during charge zinc material is transported in the opposite direction as during discharge: from the bottom towards the top of the electrode. However, since in the zinc electrode compartment the zincate concentration is much smaller during charge than during discharge, as a net result, during one cycle, zinc material is transported from the electrolyte reservoir towards the zinc electrode compartment. Note that volume variations occur also in vertical cells. Consequently, in these cells the transport of zinc material over the electrode can take place as a result of density and/or volume variations of the electrolyte. This behavior was observed in our experiments.

The shape change pattern on the zinc electrode.—From the density gradient model it can be concluded that during battery cycling zinc material is transported from the top towards the bottom of the electrode. Hence, a shape change pattern as presented in Fig. 19 is expected. This type of shape change pattern was observed indeed for electrodes cycled in a cell in which an electrolyte reservoir was present also at the bottom of the electrodes (17). This reservoir functions as a trap for electrolyte with a high density, thus increasing the deposition of zinc at the bottom of the electrode.

However, for all other cell types (17) the redistribution of zinc material over the electrode results in a shape change pattern as depicted in Fig. 20 [see *e.g.*, Fig. 8 in part I (6) and Fig. 6 in (17)]: zinc material agglomerates at the center and bottom of the electrode, and predominantly the top edges of the electrode are depleted in zinc material. The realization of this typical distribution of zinc material over the electrode can be explained with the density gradient model.

Assuming laminar flow profiles (considering the relatively low flow rates and high kinematic viscosities) the

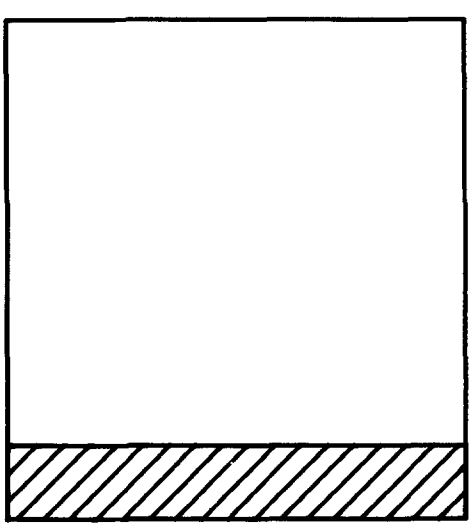

Fig. 19. Shape change pattern as expected on the basis of the density gradient model, assuming a uniform electrolyte flow over the electrode and as found experimentally for zinc electrodes cycled in cells with an electrolyte reservoir located at the bottom of the electrodes (17).

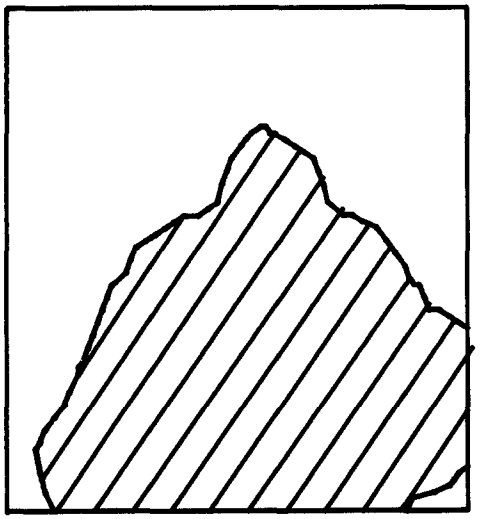

Fig. 20. Shape change pattern as expected on the basis of the density gradient model and as found experimentally for zinc electrodes cycled in other types of cell (17).

electrolyte flow in the zinc electrode compartment will be smaller at the edges than at the center of the electrode, due to adhesion of the electrolyte to the separator, which is packed more tightly around the edges than around the center of the electrode. Hence a smaller part of the amount of the zinc material displaced during discharge is retrieved during charge as compared with other regions on the electrode. Therefore, the edges of the electrode, particularly at the top, become depleted in zinc material more rapidly than other regions on the electrode, which is shown in Fig. 20.

Another aspect of the shape change pattern, only encountered in horizontal cells, is that underneath the electrode, depletion in zinc material, and above the electrode accumulation of zinc material is observed. This is also expected on the basis of the postulated model. Underneath the electrode natural convection enhances the dissolution of the zinc; but the lack of convection during charge inhibits the deposition: above the electrode natural convection enhances the electrodeposition of zinc and the lack of convection during discharge also enhances the precipitation of the anodic product on the electrode.

Conclusions

From our results, it can be inferred that the shape change phenomenon is caused by the transport of zincate ions via the battery electrolyte. The electrolyte is transported over the electrode by a convective flow. The direction of the zinc material transport has been derived from the movement of the radiotracer during the first few charge-discharge cycles. During charge the direction of the zinc material transport is opposite the direction during discharge. The amount of zinc material transported over the electrode is smaller during charge than it is during discharge. Therefore, the net zinc material transport over the electrode is in the direction as observed during discharge. Generally, the transport processes in horizontal cells are slower and the net zinc material transport rate is smaller than in vertical cells.

A new model for zinc electrode shape change is postulated: the density gradient model. In this model, the origin of shape change is the occurrence of concentration gradients during cycling of the battery. These concentration gradients are accompanied by density gradients and volume variations of the electrolyte, which induce electrolyte movement in the battery, during charge as well as during discharge. With this model the observed shape change patterns can be described, irrespective of the position of the zinc electrode in the earth's gravitational field. The model shows that, especially for zinc electrodes cycled in horizontal cells, the position and dimension of the electrolyte reservoir is of crucial importance to the extent of shape change.

Acknowledgments

The authors wish to thank Mrs. C. Zegers (IRI, Delft) for the radiochemical analysis of the many electrode samples and the Staff of the SBD (TUE, Eindhoven) for technical consultations and for assistance with the radiochemical experiments.

Manuscript submitted June 27, 1989; revised manuscript received May 13, 1990.

Eindhoven University of Technology assisted in meeting the publication costs of this article.

APPENDIX

The change in volume of the electrolyte in the zinc electrode compartment during discharge of the zinc electrode can be estimated from literature data for the density of pure KOH (12) and ZnO saturated KOH solutions (13, 14).

The procedure is as follows: after compiling, the composition of a ZnO saturated KOH solution and its density from literature data, the composition of the pure KOH solution is calculated, assuming that starting with this solution the ZnO saturated solution was formed by electrochemical discharge of zinc. Then, the weight fraction of KOH in the pure KOH solution, x_{KOH}, can be calculated from the equation

$$x_{KOH} = M_{KOH}\left(\frac{x_K}{M_K} + n_K\frac{x_{Zn}}{M_{Zn}}\right)\frac{m_2}{m_1} \qquad [A\text{-}1]$$

M_i is the molecular mass of species i, x_i its weight fraction in the ZnO saturated solution, m_1 the mass of the pure KOH solution, m_2 the mass of the ZnO saturated solution, and n_K the number of moles of K^+ transferred from the zinc electrode to the nickel electrode compartment for each zincate ion formed. The density for the pure KOH solution, ρ_1, can now be evaluated from literature data (13).

The ratio of the volume of the electrolyte in the zinc electrode compartment at the end of discharge, V_2, to the volume at the beginning of discharge, V_1, is given by

$$\frac{V_2}{V_1} = \frac{\rho_1}{\rho_2}\frac{m_2}{m_1} \qquad [A\text{-}2]$$

where ρ_2 is the density of the ZnO saturated solution.

The decrease of the total volume of the zinc electrode compartment is in fact slightly higher (about 1% more) due to the decrease in volume of the zinc electrode. The ratio of the volume decrease of the zinc electrode, V_3, to V_1 is calculated from the formula

$$\frac{V_3}{V_1} = \frac{x_{Zn}\rho_1}{\rho_3}\frac{m_2}{m_1} \qquad [A\text{-}3]$$

where ρ_3 is the density of solid zinc.

Now, assumptions have to be made about the transfer of K^+, OH^-, and H_2O from one compartment to the other (the transport of zincate is neglected because its diffusivity and mobility is low when compared with K^+ and OH^- cf. the section on The solution layer adjacent to the electrode).

Table A-I. Volume decrease during discharge for various electrolyte compositions (in the presence of a weak cationic membrane separator)

x_K[a]	x_{Zn}[a]	ρ_2[a] kg · l^{-1}	x_{KOH}	ρ_1[b] kg · l^{-1}	V_2/V_1	V_3/V_1
0.0818	0.0055	1.1076	0.1218	1.1076	0.9976	0.0009
0.1500	0.0183	1.2258	0.2291	1.2102	0.9794	0.0031
0.2130	0.0361	1.3616	0.3314	1.3139	0.9499	0.0065
0.2190	0.0371	1.3637	0.3405	1.3236	0.9550	0.0068
0.2890	0.0634	1.5356	0.4564	1.4518	0.9198	0.0125
0.2480[c]	0.0495[c]	1.4720[c]	0.3899	1.3769	0.9154	0.0093
0.2900[c]	0.0679[c]	1.5890[c]	0.4607	1.4567	0.8902	0.0135
0.2960[c]	0.0781[c]	1.6530[c]	0.4754	1.4738	0.8620	0.0156

[a] Data from (13), 25°C.
[b] Compiled from (12), 20°C.
[c] Data from (14), 18°-20°C.

Table A-II. Volume decrease during discharge for various electrolyte compositions (no membrane separator present)

x_k[a]	x_{Zn}[a]	ρ_z[a] kg · l^{-1}	x_{KOH}	ρ_l[b] kg · l^{-1}	V_2/V_1	V_3/V_1
0.0818	0.0055	1.1076	0.1201	1.1060	1.0015	0.0009
0.1500	0.0183	1.2258	0.2253	1.2065	0.9941	0.0031
0.2130	0.0361	1.3616	0.3275	1.3099	0.9812	0.0068
0.2190	0.0371	1.3637	0.3369	1.3198	0.9876	0.0070
0.2890	0.0634	1.5356	0.4576	1.4532	0.9799	0.0134
0.2480[c]	0.0495[c]	1.4720[c]	0.3875	1.3743	0.9592	0.0098
0.2900[c]	0.0679[c]	1.5890[c]	0.4622	1.4586	0.9528	0.0144
0.2960[c]	0.0781[c]	1.6530[c]	0.4784	1.4773	0.9331	0.0169

[a] Data from (13), 25°C.
[b] Compiled from (12), 20°C.
[c] Data from (14), 18°-20°C.

For example, in the presence of a weak cationic membrane separator, the transport numbers of K^+ and OH^- can be set equal (1). Assuming that along with one K^+ four water molecules are transported from the zinc electrode towards the nickel electrode compartment, the volume of the electrolyte in the zinc electrode compartment decreases significantly, as can be seen from Table A-I. If the membrane separator is omitted and only a quarter of the current is carried by K^+, a smaller decrease of the volume is observed (Table A-II).

In the actual battery system, the electrolyte in the zinc electrode compartment will not be completely depleted in zincate at the beginning of discharge. However, the electrolyte at the end of discharge will not be saturated but will be supersaturated with zincate. Furthermore, the properties of chemically and electrochemically formed zincate solutions are different (18, 19) and during discharge of the zinc electrode, apart from soluble zinc species, ZnO or related solid zinc compounds are formed. Therefore, the results in Table A-I and A-II must be taken in a qualitative sense: and it seems that in actual battery systems the volume of the electrolyte in the zinc electrode compartment decreases more than would be expected from the results in Table A-I and A-II.

REFERENCES

1. K. W. Choi, D. N. Bennion, and J. Newman, *This Journal*, **123,** 1616 (1976).
2. J. McBreen, *ibid.*, **119,** 1620 (1972).
3. K. W. Choi, D. N. Bennion, and J. Newman, *ibid.*, **123,** 1625 (1976).
4. K. W. Choi, Ph. D. Thesis, University of California, Los Angeles (1975).
5. R. G. Gunther and R. M. Bendert, *This Journal*, **134,** 782 (1987).
6. R. E. F. Einerhand, W. Visscher, J. J. M. de Goeij, and E. Barendrecht, *ibid.*, **138,** 1 (1991).
7. R. E. F. Einerhand, W. H. M. Visscher, E. Barendrecht, and J. J. M. de Goeij, p. 751 of Extended Abstracts of 38th ISE Meeting," Vol. 2, Maastricht, 1987.
8. E. H. Hietbrink and R. F. Hill, *This Journal*, **136,** 310 (1989).
9. J. McBreen and E. J. Cairns, in "Advances in Electrochemistry and Electrochemical Engineering," Vol. 11, H. Gerischer and C. W. Tobias, Editors, p. 273, John Wiley & Sons, Inc., New York (1978).
10. K. W. Choi, D. Hamby, D. N. Bennion, and J. Newman, *This Journal*, **123,** 628 (1976).
11. R. E. F. Einerhand, Ph.D. Thesis, Eindhoven University of Technology, Eindhoven (1989).
12. "Handbook of Chemistry and Physics," 62nd ed., CRC Press Inc., Boca Raton, FL (1981-1982).
13. T. P. Dirkse, *This Journal*, **106,** 154 (1959).
14. V. G. Sochevanov, *J. Gen. Chem. U.S.S.R.*, **22,** 1119 (1952).
15. D. C. Hamby, N. J. Hoover, J. Wirkkala, and D. Zahnle, *This Journal*, **126,** 2110 (1979).
16. M. J. Isaacson, F. R. McLarnon, and E. J. Cairns, Abstract 147, p. 214, The Electrochemical Society Extended Abstracts, Vol. 87-2, Honolulu, HI, Oct. 18-23, 1987.
17. R. E. F. Einerhand, Ph.D. Thesis, Chap. 5, pp. 83-98, Eindhoven University of Technology, Eindhoven (1989).
18. C. Cachet, B. Saidani, and R. Wiart, *Electrochim. Acta.*, **33,** 405 (1988).
19. V. E. Dmitrenko, M. S. Zukov, V. I. Baulov, and A. V. Kotov, *Sov. Electrochem.*, **19,** 1414 (1983).

A Mathematical Model of a Sealed Nickel-Cadmium Battery

Deyuan Fan* and Ralph E. White**

Department of Chemical Engineering, Texas A&M University, College Station, Texas 77843-3122

ABSTRACT

A mathematical model for the charge and discharge of a sealed nickel-cadmium (Ni-Cd) battery is presented. The model is used to study the effect of transport properties of the electrolyte and kinetic parameters of the electrode reactions on the cell performance during the charge and discharge period. The model can also be used to demonstrate the changes of cell performance during cycling. Some comparisons between model predictions and experimental results indicate that the model predictions appear to fit the experimental data well. Sensitivity analyses illustrate that the sealed nickel-cadmium battery operates under activation control. It is also shown theoretically that oxygen generated on the positive electrode during charge is reduced electrochemically on the negative electrode.

It is well known that the performance of a nickel-cadmium battery is based on the complex chemical and electrochemical phenomena (1-4) involved in the battery. These complex phenomena can be understood better through mathematical modeling of the battery. Similar work has been done for other battery systems such as the model for the nickel-zinc battery by Choi and Yao (5) and the model for the lead-acid battery by Gu *et al.* (6), both for flooded/vent conditions. In October 1989, Bouet and Richard (7) presented their discharge performance model for the nickel hydroxide electrode at the 176th Meeting of The Electrochemical Society. However, their model includes only the nickel positive electrode and does not include sealed cell conditions and the oxygen reaction. Recently, Nguyen *et al.* (8) proposed a mathematical model for the lead-acid battery under sealed conditions during discharge, but a model for predicting the cell performance under sealed conditions during charge has not been presented. To assist researchers and designers in the investigation and development of sealed nickel-cadmium batteries, a detailed mathematical model of a sealed, starved separator nickel-cadmium cell is presented here that can be used to predict the performance of a cell not only during discharge, but also during charge, rest, and cycling. A description of the model equations, qualitative comparisons between the model predictions and experimental re-

* Electrochemical Society Student Member.
** Electrochemical Society Active Member.